Formation Control in a Leader-Fixed Frame for Agents with Extended Unicycle Dynamics that Include Orientation Kinematics on SO(m)

Christopher Heintz and Jesse B. Hoagg

Abstract—We present a formation control algorithm for agents with extended unicycle dynamics that include orientation kinematics on SO(m) and first-order speed dynamics. The desired interagent positions are expressed in a leader-fixed coordinate frame, which is aligned with and rotates with the leader's velocity vector. Thus, the desired interagent positions vary in time as the leader-fixed frame rotates. We assume that each agent has relative-position feedback of its neighbor agents, where the neighbor sets are such that the interagent communication (i.e., feedback) structure represents a strongly connected directed graph. We assume that at least one agent has access to a measurement its position relative to the leader. The analytic result shows that for almost all initial conditions, the agents converge to the desired relative positions. We also present results from software-in-the-loop simulations with 3 fixed-wing unmanned air vehicles (UAVs) that demonstrate the leader-fixed formation-control algorithm.

I. INTRODUCTION

Autonomous multi-vehicle systems have a variety applications such as distributed sensing [1], cooperative surveillance [2], precision agriculture, and search and rescue. For coordinated formation control, each agent typically relies on sensing or interagent communication to determine necessary feedback information (e.g., interagent positions). Then, each agent uses this feedback information in combination with feedforward information (e.g., external commands, mission objectives) to accomplish tasks such as collision avoidance, cohesion, guidance, and velocity matching.

Consensus algorithms have been extended to address cohesion and collision avoidance (e.g., [3]–[6]). These approaches force agents into a predetermined formation by specifying the desired relative position between pairs of agents. Other examples of formation control algorithms include [7]–[17]. Surveys of multi-agent formation-control methods are presented in [18]–[20]. Experimental demonstrations of formation-control algorithms include [2], [13], [21]–[26]. In particular, [2], [23]–[25] present formation-control experiments with fixed-wing UAVs. Simulation results on formation-control for fixed-wing UAVs are also provided in [27]–[30].

This paper addresses formation control in a leader-fixed frame for agents with extended unicycle dynamics that include orientation kinematics on SO(m) and first-order speed dynamics. Related models are used in [9], [13], [24], [27], [29], [31]–[33], but these models do not include orientation kinematics on SO(m). The desired interagent positions are

This work is supported in part by the National Science Foundation (OIA-1539070) and the National Aeronautics and Space Administration (NNX15AR69H) through the NASA Kentucky Space Grant.

expressed in a leader-fixed coordinate frame, which is aligned with the leader's velocity vector. The leader can be a physical agent or a virtual agent. The algorithm in this paper applies to formations where: i) the neighbor sets are such that the interagent communication structure represents a strongly connected directed graph; ii) at least one agent has access to a measurement its position relative to the leader; and iii) each agent also has feedforward of the leader's velocity, acceleration, and orientation and its first two derivatives. The main analytic result shows that for almost all initial conditions, the agents converge to the desired relative positions. Note that topological constraints associated with SO(m) prevent global convergence using a continuous control [34].

We also present results from software-in-the-loop (SITL) simulations with 3 fixed-wing UAVs that demonstrate the leader-fixed formation-control algorithm. In these SITL simulations the agent UAVs maintain a desired formation as the leader performs course maneuvers. To implement the formation-control algorithm, we use middle-loop controllers, which accept as commands the controls computed by the formation control algorithm. A Pixhawk autopilot provides inner-loop attitude stabilization.

II. PROBLEM FORMULATION

Let the positive number n be the number of agents, and define the agent index set $\mathcal{I} \triangleq \{1,2,\ldots,n\}$. Define $\mathcal{P} \triangleq \{(i,j) \in \mathcal{I} \times \mathcal{I} : i \neq j\}$, which is the set of ordered pairs. Unless otherwise stated, all statements that involve the subscript i are for all $i \in \mathcal{I}$.

For clarity of presentation, we first develop the extended unicycle model in three-dimensional space. Thus, for the moment, let m=3.

Let E be an inertial frame (e.g., the Earth frame), and let $o_{\rm E}$ be the origin of E. Let o_i be the location of the ith agent (e.g., the location of the ith vehicle's center of mass). The position of o_i relative to $o_{\rm E}$ is $\overrightarrow{q_i}$, and the ith agent's position $\overrightarrow{q_i}$ is resolved in E as $q_i \triangleq \overrightarrow{q_i}|_{\rm E}$. The velocity of o_i relative to $o_{\rm E}$ with respect to E is $\overrightarrow{p_i} \triangleq^{\rm E} \cdot \overrightarrow{q_i}$. Let B_i be a frame that is fixed to o_i such that $\overrightarrow{p_i}$ resolved in B_i is given by $\overrightarrow{p_i}|_{B_i} = s_i v_i$, where $v_i \in \mathbb{R}^m$ is a unit vector and for all $t \geq 0$, $s_i(t) \in \mathbb{R}$ is the speed of the ith agent. Let $R_i : [0, \infty) \to {\rm SO}(m)$ be the rotation matrix from B_i to E. Thus, the ith agent's velocity $\overrightarrow{p_i}$ resolved in E is $\overrightarrow{p_i}|_{\rm E} = s_i R_i v_i$, which implies that

$$\dot{q}_i(t) = s_i(t)R_i(t)v_i,\tag{1}$$

where $t \geq 0$; $q_i(t) \in \mathbb{R}^m$, $s_i(t) \in \mathbb{R}$, and $R_i^{\mathrm{T}}(t) \in \mathrm{SO}(m)$ are the position, speed, and orientation of the *i*th agent; and $q_i(0) \in \mathbb{R}^m$ is the initial condition. Note that for all $t \geq 0$,

C. Heintz and J. B. Hoagg are with the Department of Mechanical Engineering, University of Kentucky, Lexington, KY, USA. (e-mail: cmhe234@g.uky.edu, jesse.hoagg@uky.edu).

 $R_i(t)v_i$ is unit vector in the direction of the velocity $\dot{q}_i(t)$. The speed and orientation of the *i*th agent satisfy

$$\dot{s}_i(t) = f_i(s_i(t), R_i(t)) + g_i(s_i(t), R_i(t))u_i(t), \quad (2)$$

$$\dot{R}_i(t) = R_i(t)\Omega_i(t),\tag{3}$$

where $t \geq 0$; $u_i : [0, \infty) \to \mathbb{R}$ and $\Omega_i : [0, \infty) \to \operatorname{so}(m)$ are the control inputs; $s_i(0) \in \mathbb{R}$ and $R_i(0) \in \operatorname{SO}(m)$ are the initial conditions; and $f : [0, \infty) \times \operatorname{SO}(m) \to \mathbb{R}$ and $g : [0, \infty) \times \operatorname{SO}(m) \to \mathbb{R} \setminus \{0\}$. Note that Ω_i is the skew-symmetric form of the angular velocity of B_i relative to E resolved in B_i . The agent model (1)–(3) is an extended unicycle model that includes both speed dynamics (2) and orientation kinematics (3) on $\operatorname{SO}(m)$.

Let $o_{\rm g}$ be the location of the leader, which can be a physical agent (e.g., a vehicle) or a virtual agent. The position of $o_{\rm g}$ relative to $o_{\rm E}$ is $\overrightarrow{q_{\rm g}}$, and the leader's position $\overrightarrow{q_{\rm g}}$ is resolved in E as $q_{\rm g} \triangleq \overrightarrow{q_{\rm g}}|_{\rm E}$, which is assumed to be twice continuously differentiable. The velocity of $o_{\rm g}$ relative to $o_{\rm E}$ with respect to E is $\overrightarrow{p_{\rm g}} \triangleq^{\rm E} \overrightarrow{q_{\rm g}}$. Let $B_{\rm g}$ be a frame that is fixed to $o_{\rm g}$ and has orthogonal unit vectors $\hat{\imath}_{\rm g}$, $\hat{\jmath}_{\rm g}$, and $\hat{k}_{\rm g}$, where $\hat{\imath}_{\rm g}$ is parallel to the leader's velocity vector $\overrightarrow{p_{\rm g}}$, and the rotation matrix from $B_{\rm g}$ to E is $R_{\rm g}:[0,\infty)\to {\rm SO}(m)$, which is assumed to be twice continuously differentiable.

In this paper, we address the problem of formation control in the leader-fixed frame B_g . Let $d_i \in \mathbb{R}^m$ be the desired position of o_i relative to o_g resolved in B_g . Thus, for all $(i,j) \in \mathcal{P}$, $d_{ij} \triangleq d_i - d_j$ is the desired position of o_i relative to o_j resolved in B_g . Our objective is to design controls u_i and Ω_i such that:

- (O1) For all $(i, j) \in \mathcal{P}$, $\lim_{t \to \infty} R_{g}^{T}(t)[q_{i}(t) q_{j}(t)] = d_{ij}$. (O2) For all $i \in \mathcal{I}$, $\lim_{t \to \infty} [\dot{q}_{i}(t) - \dot{q}_{g}(t) - \dot{R}_{g}(t)d_{i}] = 0$.
- (O3) For all $i \in \mathcal{I}$, $\lim_{t\to\infty} R_g^T(t)[q_i(t) q_g(t)] = d_i$.

Objective (O1) states that each agent approaches its desired relative positions with the other agents. Objective (O2) states that each agent's velocity with respect to $B_{\rm g}$ approaches the leader's velocity with respect to $B_{\rm g}$. Objective (O3) states that each agent approaches its desired relative position with the leader. Note that if (O3) is satisfied, then (O1) is satisfied. However, we enumerate these objectives independently because some results in this paper show that it is possible to satisfy (O1) but not (O3) under weaker interagent communication assumptions.

Although the physical (i.e., frame-based) formulation of the formation control problem is described in three dimensions, the methods in this paper apply to all $m \in \{2,3,4,\ldots\}$. For example, m=2 is for planar motion. Thus, for the remainder of this paper, we consider the extended unicycle model (1)–(3) and the objectives (O1)–(O3), where $m \in \{2,3,4,\ldots\}$.

The interagent communication (i.e., feedback) structure is represented using a directed graph. The agent index set \mathcal{I} is the *vertex set* of the directed graph, and the n elements of \mathcal{I} are the *vertices*. Let $\mathcal{E} \subset \mathcal{I} \times \mathcal{I}$ be the *directed edge set*. The elements of \mathcal{E} are the *directed edges*. Then, the directed graph is $\mathcal{G} = (\mathcal{I}, \mathcal{E})$. The directed graph $\mathcal{G} = (\mathcal{I}, \mathcal{E})$ has a walk of length l from $v_0 \in \mathcal{I}$ to $v_l \in \mathcal{I}$ if there exists an (l+1)-tuple $(v_0, v_1, \ldots, v_l) \in \mathcal{I} \times \mathcal{I} \times \cdots \times \mathcal{I}$ such that

for all $j \in \{1, 2, ..., l\}$, $(v_{j-1}, v_j) \in \mathcal{E}$. The directed graph $\mathcal{G} = (\mathcal{I}, \mathcal{E})$ is *strongly connected* if for all distinct $i, j \in \mathcal{I}$, there exists a walk from i to j.

Define the neighbor set $N_i \triangleq \{j \in \mathcal{I} : (j,i) \in \mathcal{E}\}$. We assume that for all $i \in \mathcal{I}$, $(i,i) \in \mathcal{E}$, which implies that $i \in \mathcal{N}_i$. We assume that $\mathcal{G} = (\mathcal{I}, \mathcal{E})$ is strongly connected, and the ith agent has access to $\{q_j\}_{j \in \mathcal{N}_i}$ and $\{\dot{q}_j\}_{j \in \mathcal{N}_i}$ for feedback. In addition, we assume that each agent has access to measurements of the leader's velocity \dot{q}_g , the leader's acceleration \ddot{q}_g , and R_g , \dot{R}_g , and \ddot{R}_g for feedforward. However, the formation control algorithm presented in this paper only requires that at least one agent has access to a measurement of q_g .

III. FORMATION CONTROL ALGORITHM

Define the ith agent's desired velocity

$$p_{d,i} \triangleq \dot{q}_{g} + \dot{R}_{g}d_{i} + \alpha_{i}(q_{g} - q_{i} + R_{g}d_{i}) + \sum_{j \in \mathcal{N}_{i}} \beta_{ij}(q_{j} - q_{i} + R_{g}d_{ij}), \tag{4}$$

where $\alpha_i \geq 0$, for all $j \in \mathcal{N}_i \setminus \{i\}$, $\beta_{ij} > 0$, and for all $j \notin \mathcal{N}_i \setminus \{i\}$, $\beta_{ij} = 0$. Note that the *i*th agent's desired velocity depends on a measurement of q_g if and only if $\alpha_i > 0$. The formation control algorithm in this paper only requires that there exists $l \in \mathcal{V}$ such that $\alpha_l > 0$, that is, at least one agent has access to a measurement of q_g .

Define the desired speed

$$s_{\mathrm{d},i} \triangleq ||p_{\mathrm{d},i}||,\tag{5}$$

where $\|\cdot\|$ denotes the 2-norm. For simplicity, we make the technical assumption that the leader's translational and rotational trajectories (i.e., $q_{\rm g}$, $\dot{q}_{\rm g}$, $R_{\rm g}$, and $\dot{R}_{\rm g}$) are such that the desired speed is bounded away from zero. Specifically, we make the following assumption:

(A1) There exists $\varepsilon > 0$ such that for all $t \ge 0$, $s_{\mathrm{d},i}(t) > \varepsilon$. Next, consider the formation control

$$u_{i} = \frac{1}{g_{i}(s_{i}, R_{i})} \left[\dot{s}_{d,i} - f_{i}(s_{i}, R_{i}) - \gamma_{i}(s_{i} - s_{d,i}) \right], \quad (6)$$

$$\Omega_{i} = \eta_{i} s_{d,i} \left(R_{i}^{T} p_{d,i} v_{i}^{T} - v_{i} p_{d,i}^{T} R_{i} \right)$$

$$+ \frac{1}{s_{d,i}^{T}} R_{i}^{T} \left(\dot{p}_{d,i} p_{d,i}^{T} - p_{d,i} \dot{p}_{d,i}^{T} \right) R_{i}, \quad (7)$$

where $\gamma_i > 0$, $\eta_i > 0$, and

$$\dot{p}_{d,i} \triangleq \ddot{q}_{g} + \ddot{R}_{g}d_{i} + \alpha_{i} \Big(\dot{q}_{g} - \dot{q}_{i} + \dot{R}_{g}d_{i} \Big)$$

$$+ \sum_{j \in \mathcal{N}_{i}} \beta_{ij} \Big(\dot{q}_{j} - \dot{q}_{i} + \dot{R}_{g}d_{ij} \Big), \tag{8}$$

$$\dot{s}_{\mathrm{d},i} \triangleq \frac{\partial s_{\mathrm{d},i}}{\partial p_{\mathrm{d},i}} \dot{p}_{\mathrm{d},i} = \frac{1}{s_{\mathrm{d},i}} p_{\mathrm{d},i}^{\mathrm{T}} \dot{p}_{\mathrm{d},i}. \tag{9}$$

Note that (A1) guarantees that u_i and Ω_i are well defined.

IV. STABILITY ANALYSIS

In this section, we analyze the closed-loop dynamics (1)–(9). Define the position error $\zeta_i \triangleq q_i - q_{\rm g} - R_{\rm g} d_i$, and differentiating and using (1) implies that

$$\dot{\zeta}_i = p_{d,i} - p_{d,i} + s_i R_i v_i - \dot{q}_g - \dot{R}_g d_i.$$
 (10)

Substituting (4) into (10) yields

$$\dot{\zeta}_i = -\alpha_i \zeta_i + s_i R_i v_i - p_{d,i} + \sum_{j \in \mathcal{N}_i} \beta_{ij} (\zeta_j - \zeta_i).$$
 (11)

Define $\zeta(t) \triangleq [\zeta_1^{\mathrm{T}}(t) \quad \cdots \quad \zeta_n^{\mathrm{T}}(t)]^{\mathrm{T}} \in \mathbb{R}^{mn}$, and it follows from (11) that

$$\dot{\zeta} = -[(A+L) \otimes I_m]\zeta + \sum_{i \in \mathcal{I}} (E_i \otimes I_m)(s_i R_i v_i - p_{d,i}),$$
(12)

where

$$A \triangleq \operatorname{diag}(\alpha_1, \dots, \alpha_n) \in \mathbb{R}^{n \times n},$$

$$E_i \triangleq \begin{bmatrix} 0_{1 \times i-1} & 1 & 0_{1 \times n-i} \end{bmatrix}^{\mathrm{T}} \in \mathbb{R}^n,$$

and for all $(i,j) \in \mathcal{P}$, the (i,j)th element of $L \in \mathbb{R}^{n \times n}$ is $E_i^{\mathrm{T}} L E_j = -\beta_{ij}$, for all $i \in \mathcal{I}$, the (i,i)th element of $L \in \mathbb{R}^{n \times n}$ is $E_i^{\mathrm{T}} L E_i = \sum_{j \in \mathcal{N}_i} \beta_{ij}$, and $\mathrm{diag}(\cdot)$ is a diagonal matrix whose diagonal elements are given by the arguments of the operator. Note that L is the Laplacian of the directed graph $\mathcal{G} = (\mathcal{I}, \mathcal{E})$, where for all $(i,j) \in \mathcal{E}$, we associate the weight β_{ij} .

Let $1_n \in \mathbb{R}^n$ denote the $n \times 1$ vector of ones. The following result, which is from [35], is used to analyze stability.

Lemma 1. Assume that $\mathcal{G} = (\mathcal{I}, \mathcal{E})$ is strongly connected. Then, there exists a positive-definite diagonal matrix $D \in \mathbb{R}^{n \times n}$ such that the following statements hold:

- i) $DL + L^{T}D$ is positive semidefinite.
- ii) 0 is a simple eigenvalue of $DL + L^{T}D$ and $(DL + L^{T}D)1_{n} = 0$.

Consider $V_0:\mathbb{R}^{mn}\to [0,\infty)$ defined by $V_0(\zeta)\triangleq \zeta^{\mathrm{T}}(D\otimes I_m)\zeta$, where $D\in\mathbb{R}^{n\times n}$ is the positive-definite diagonal matrix given by Lemma 1, which exists because $\mathcal{G}=(\mathcal{I},\mathcal{E})$ is strongly connected. The following preliminary result considers the case where the velocity $s_iR_iv_i$ is a control variable. Specifically, this result addresses the case where $s_iR_iv_i=p_{\mathrm{d},i}$. The proof is omitted for space considerations.

Proposition 1. Consider the closed-loop dynamics (12), which consists of (1) and (4), where $s_i R_i v_i = p_{\mathrm{d},i}$. Assume that $\mathcal{G} = (\mathcal{I}, \mathcal{E})$ is strongly connected. Then, the following statements hold:

- i) $\dot{V}_0(\zeta) \triangleq \frac{\partial V_0(\zeta)}{\partial \zeta} \dot{\zeta} = -\zeta^{\mathrm{T}}[(DL + L^{\mathrm{T}}D + 2DA) \otimes I_m]\zeta$ is negative semidefinite.
- ii) The equilibrium $\zeta(t) \equiv 0$ of (12) is a Lyapunov stable.
- iii) For all $i \in \mathcal{I}$ and $q_i(0) \in \mathbb{R}^n$, (O1) and (O2) are satisfied.
- iv) If there exists $l \in \mathcal{I}$ such that $\alpha_l > 0$, then $DL + L^TD + 2DA$ is positive definite and for all $i \in \mathcal{I}$ and $q_i(0) \in \mathbb{R}^n$, (O3) is satisfied.

Proposition 1 shows that if $s_i R_i v_i = p_{\mathrm{d},i}$ and there exists $l \in \mathcal{I}$ such that $\alpha_l > 0$ (i.e., at least one agent has a measurement of q_{g}), then (O1)–(O3) are satisfied. However, the speed s_i and pointing direction $R_i v_i$ are not controls. Instead, s_i is determined from (2), which has control input

 u_i , and $R_i v_i$ is determined from (3), which has control input Ω_i . We now analyze the full closed-loop dynamics (1)–(9).

Define the desired pointing direction $b_{d,i} \triangleq \frac{1}{s_{d,i}} p_{d,i}$, and define the speed and pointing direction errors

$$\tilde{s}_i \stackrel{\triangle}{=} s_i - s_{\mathrm{d},i},\tag{13}$$

$$\tilde{b}_i \triangleq R_i v_i - b_{\mathrm{d},i}. \tag{14}$$

Next, note that $s_i R_i v_i - p_{d,i} = \tilde{s}_i R_i v_i + s_{d,i} \tilde{b}_i$. Thus, it follows from (12) that

$$\dot{\zeta} = -[(A+L) \otimes I_m]\zeta + \sum_{i \in \mathcal{I}} (E_i \otimes I_m) \Big(\tilde{s}_i R_i v_i + s_{\mathrm{d},i} \tilde{b}_i \Big).$$
(15)

Differentiating (13) and using (2) and (6) implies

$$\dot{\tilde{s}}_i = f_i(s_i, R_i) + g_i(s_i, R_i)u_i - \dot{s}_d = -\gamma_i \tilde{s}_i,$$
 (16)

Similarly, differentiating (14) and using (3) and (7) implies

$$\dot{\hat{b}}_i = \eta_i s_{\mathrm{d},i} \left(p_{\mathrm{d},i} v_i^{\mathrm{T}} v_i - R_i v_i p_{\mathrm{d},i}^{\mathrm{T}} R_i v_i \right)
+ \frac{1}{s_{\mathrm{d},i}^2} \left(\dot{p}_{\mathrm{d},i} p_{\mathrm{d},i}^{\mathrm{T}} - p_{\mathrm{d},i} \dot{p}_{\mathrm{d},i}^{\mathrm{T}} \right) R_i v_i - \dot{b}_{\mathrm{d},i}.$$

Since $p_{d,i} = s_{d,i} b_{d,i}$, $\dot{p}_{d,i} = \dot{s}_{d,i} b_{d,i} + s_{d,i} \dot{b}_{d,i}$, $v_i^T v_i = 1$, and $b_{d,i} = -\tilde{b}_i + R_i v_i$, it follows that

$$\begin{split} \dot{\tilde{b}}_i &= \eta_i s_{\mathrm{d},i}^2 \Big(-\tilde{b}_i + \left(1 - b_{\mathrm{d},i}^\mathrm{T} R_i v_i \right) R_i v_i \Big) \\ &- \dot{b}_{\mathrm{d},i} \big(1 - b_{\mathrm{d},i}^\mathrm{T} R_i v_i \big) - b_{\mathrm{d},i} \dot{b}_{\mathrm{d},i}^\mathrm{T} R_i v_i. \end{split}$$

Since $b_{\mathrm{d},i}$ is a unit vector, it follows that $\dot{b}_{\mathrm{d},i}^{\mathrm{T}}b_{\mathrm{d},i}=0$. In addition, note that $1-b_{\mathrm{d},i}^{\mathrm{T}}R_{i}v_{i}=\frac{1}{2}\tilde{b}_{i}^{\mathrm{T}}\tilde{b}_{i}$ and $R_{i}v_{i}=\tilde{b}_{i}+b_{\mathrm{d},i}$. Thus,

$$\dot{\tilde{b}}_{i} = -\eta_{i} s_{\mathrm{d},i}^{2} \left(\tilde{b}_{i} - \frac{1}{2} \tilde{b}_{i}^{\mathrm{T}} \tilde{b}_{i} \left(\tilde{b}_{i} + b_{\mathrm{d},i} \right) \right) - \frac{1}{2} \dot{b}_{\mathrm{d},i} \tilde{b}_{i}^{\mathrm{T}} \tilde{b}_{i}
- b_{\mathrm{d},i} \dot{b}_{\mathrm{d},i}^{\mathrm{T}} \tilde{b}_{i}.$$
(17)

Next, define

$$Q \triangleq \{(\{q_i\}_{i \in \mathcal{I}}, \{s_i\}_{i \in \mathcal{I}}, \{R_i\}_{i \in \mathcal{I}}) \in \mathbb{R}^{mn} \times \mathbb{R}^n \times SO(m)^n : \text{ for all } i \in \mathcal{I}, b_{\mathbf{d}_i}^{\mathbf{d}_i}(0) R_i v_i \neq -1\},$$

which is the set of initial conditions such that the angle from initial velocity $\dot{q}_i(0)$ to the initial desired velocity $p_{\mathrm{d},i}(0)$ is not exactly π rad.

The following theorem is the main analytic result of this paper. This result demonstrates that the equilibrium $(\zeta(t), \{\tilde{s}_i(t)\}_{i\in\mathcal{I}}, \{\tilde{b}_i(t)\}_{i\in\mathcal{I}}) \equiv (0,0,0)$ of the closed-loop system (15)–(17) is almost globally asymptotically stable, and for almost all initial conditions, (O1)–(O3) are satisfied. Note that topological constraints associated with SO(m) prevent global asymptotic stability of the equilibrium using a continuous control [34]. The proof is omitted for space considerations.

Theorem 1. Consider the closed-loop dynamics (15)–(17), which consists of (1)–(9), where (A1) is satisfied. Assume that $\mathcal{G} = (\mathcal{I}, \mathcal{E})$ is strongly connected, and assume that there exists $l \in \mathcal{I}$ such that $\alpha_l > 0$. Then, the equilibrium $(\zeta(t), \{\tilde{s}_i(t)\}_{i \in \mathcal{I}}, \{\tilde{b}_i(t)\}_{i \in \mathcal{I}}) \equiv (0, 0, 0)$ of (15)–

(17) is Lyapunov stable. Furthermore, for all initial conditions $(\{q_i(0)\}_{i\in\mathcal{I}}, \{s_i(0)\}_{i\in\mathcal{I}}, \{R_i(0)\}_{i\in\mathcal{I}}) \in \mathcal{Q}$, the following statements hold:

- i) For all $i \in \mathcal{I}$ and for all $t \geq 0$, $b_{d,i}^{T}(t)R_i(t)v_i > -1$.
- ii) For all $i \in \mathcal{I}$, $\lim_{t \to \infty} \zeta_i(t) = 0$, $\lim_{t \to \infty} \tilde{s}_i(t) = 0$, and $\lim_{t \to \infty} \tilde{b}_i(t) = 0$.
- iii) (O1)-(O3) are satisfied.

Next, we present two specializations of Theorem 1, which address the cases where either the speed s_i or the pointing direction $R_i v_i$ are control variables. Note that Proposition 1 addresses the case where both speed s_i and the pointing direction $R_i v_i$ are control variables.

Theorem 2. Consider the closed-loop dynamics (15) and (17), which consists of (1), (3)–(5), (7), and (8), where $s_i = s_{\mathrm{d},i}$ and (A1) is satisfied. Assume that $\mathcal{G} = (\mathcal{I}, \mathcal{E})$ is strongly connected, and assume that there exists $l \in \mathcal{I}$ such that $\alpha_l > 0$. Then, the equilibrium $(\zeta(t), \{\tilde{b}_i(t)\}_{i \in \mathcal{I}}) \equiv (0,0)$ of (15) and (17) with $s_i = s_{\mathrm{d},i}$ is Lyapunov stable. Furthermore, for all $i \in \mathcal{I}$ and all $(q_i(0), R_i(0)) \in \mathbb{R}^m \times \mathrm{SO}(m)$ such that $b_{\mathrm{d},i}^{\mathrm{T}}(0)R_i(0)v_i \neq -1$, the following statements hold:

- i) For all $i \in \mathcal{I}$ and for all $t \geq 0$, $b_{d,i}^{T}(t)R_i(t)v_i > -1$.
- ii) For all $i \in \mathcal{I}$, $\lim_{t \to \infty} \zeta_i(t) = 0$ and $\lim_{t \to \infty} \tilde{b}_i(t) = 0$.
- iii) (O1)-(O3) are satisfied.

Theorem 3. Consider the closed-loop dynamics (15) and (16), which consists of (1), (2), (4)–(6), (8), and (9), where $R_i v_i = b_{\mathrm{d},i}$ and (A1) is satisfied. Assume that $\mathcal{G} = (\mathcal{I}, \mathcal{E})$ is strongly connected, and assume that there exists $l \in \mathcal{I}$ such that $\alpha_l > 0$. Then, the equilibrium $(\zeta(t), \{\tilde{s}_i(t)\}_{i \in \mathcal{I}}) \equiv (0,0)$ of (15) and (16) with $R_i v_i = b_{\mathrm{d},i}$ is Lyapunov stable. Furthermore, for all $i \in \mathcal{I}$ and all $(q_i(0), s_i(0)) \in \mathbb{R}^m \times \mathbb{R}$, the following statements hold:

- i) For all $i \in \mathcal{I}$, $\lim_{t \to \infty} \zeta_i(t) = 0$ and $\lim_{t \to \infty} \tilde{s}_i(t) = 0$.
- ii) (O1)-(O3) are satisfied.

V. NUMERICAL RESULTS

For all examples in this section, let n=3 agents, and let m=3. For all $i\in\{1,2,\ldots,m\}$, define $e_i\triangleq[0_{1\times i-1}\quad 1\quad 0_{1\times m-i}]^{\rm T}\in\mathbb{R}^m$. Let $v_i=e_1$, which implies that each agent's velocity is in the body-fixed e_1 -direction. Let $f_i(s_i,R_i)=-0.4s_i$ and $g_i(s_i,R_i)=0.4$, which implies that the speed dynamics are low pass with unity gain at dc.

The desired positions are $d_1 = \begin{bmatrix} -5 & 5 & 1 \end{bmatrix}^T$ m, $d_2 = \begin{bmatrix} -5 & -5 & 2 \end{bmatrix}^T$ m, and $d_3 = \begin{bmatrix} -10 & -10 & 3 \end{bmatrix}^T$ m. Let $\mathcal{N}_1 = \{1,3\}$, $\mathcal{N}_2 = \{1,2\}$, and $\mathcal{N}_3 = \{2,3\}$, which represents a cyclic feedback structure. For all $j \in \mathcal{N}_i \setminus \{i\}$, let $\beta_{ij} = 0.6$, and let $\alpha_1 = 2$ and $\alpha_2 = \alpha_3 = 0$, which implies that only the first agent has access to a measurement of q_g . Let $\gamma_i = 1$ and $\eta_i = 0.01$.

We present numerical examples where the formation control algorithm (4)–(9) is implemented with sampled data. All feedback is sampled with sample time $T_{\rm s}=0.05~{\rm s}$, and a zero-order hold is applied to the control inputs Ω_i and u_i .

For convenience in describing the rotation $R_{\rm g}$, let $\psi_{\rm g}$, $\theta_{\rm g}$, and $\phi_{\rm g}$ be the yaw, pitch, and roll Euler angles of a 3-2-1

rotation sequence, which rotates E to Bg. Thus, $R_{\rm g}$ can be parameterized by $\psi_{\rm g}$, $\theta_{\rm g}$, and $\phi_{\rm g}$.

The sampled-data measurements of $\dot{\psi}_{\rm g}$, $\dot{\theta}_{\rm g}$, $q_{\rm g}$, and q_i are corrupted by zero-mean Gaussian white noise with variances $4 \times 10^{-4} \, {\rm rad^2/s^2}$, $4 \times 10^{-4} \, {\rm rad^2/s^2}$, $0.25 \, {\rm m^2}$, and $0.25 \, {\rm m^2}$.

Example 1. The leader's initial position is $q_{\rm g}(0)=0$ m, and its velocity is $\dot{q}_{\rm g}(t)=10R_{\rm g}(t)e_1$ m/s, where $\psi_{\rm g}(t)=0.1t,~\theta_{\rm g}(t)\equiv0,$ and $\phi_{\rm g}(t)\equiv0.$ The agents start with randomly selected initial positions and orientations, and $s_i(0)=18$ m/s. Figure 1 shows the desired $R_{\rm g}d_i$ and actual $q_i-q_{\rm g}$ relative positions in the $e_1,~e_2,$ and e_3 directions. Note that the desired relative positions $R_{\rm g}d_i$ are not constant because the leader's orientation changes with time. The relative positions converge to the desired values by approximately t=10 s. After t=10 s, the root-mean-square (RMS) magnitude $\|\zeta_i\|$ of the position errors are 0.057 m, 0.103 m, and 0.080 m for agent 1, 2, and 3, respectively. \triangle

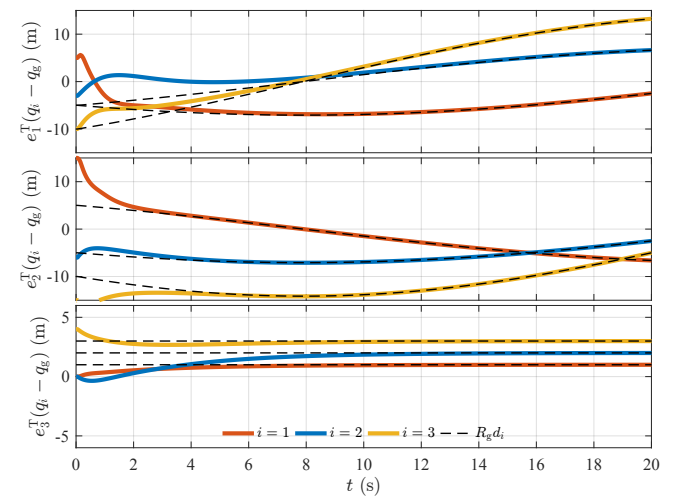


Fig. 1. Desired and actual relative positions of agents with respect to leader. Desired relative positions are achieved by approximately $t=10~\mathrm{s}$.

Example 2. The leader's initial position is $q_{\rm g}(0)=0$ m, and its velocity is $\dot{q}_{\rm g}(t)=10R_{\rm g}e_1$ m/s, where $\psi_{\rm g}(t)=0.1t+0.2\cos\pi t$, $\theta_{\rm g}(t)=0.2\cos0.2\pi$, and $\phi_{\rm g}(t)\equiv0$. The agents start with randomly selected initial positions and orientations, and $s_i(0)=18$ m/s. Figure 2 shows $R_{\rm g}d_i$ and $q_i-q_{\rm g}$. The relative positions converge to the desired values by approximately t=10 s. After t=10 s, the RMS magnitude $\|\zeta_i\|$ of the position errors are 0.069 m, 0.105 m, and 0.094 m for agent 1, 2, and 3, respectively.

These numerical examples illustrate that the control (4)–(9) approximately achieves the objectives (O1)–(O3) with sampled data and sensor noise. If the sensor noise is removed and the sample time approaches zero, then the average power of the position errors tends to zero in both examples.

VI. APPLICATION TO FIXED-WING UAVS

We apply the formation control algorithm (4)–(9) to fixedwing UAVs, where $v_i = e_1$. Let ψ_i , θ_i , and ϕ_i be the Euler angles of a 3-2-1 rotation sequence, which rotates E to B_i. Thus, R_i is parameterized by ψ_i , θ_i , and ϕ_i . Let $\hat{\psi}_i$, $\hat{\theta}_i$, and $\hat{\phi}_i$ denote the yaw, pitch, and roll of the aircraft. In the absence

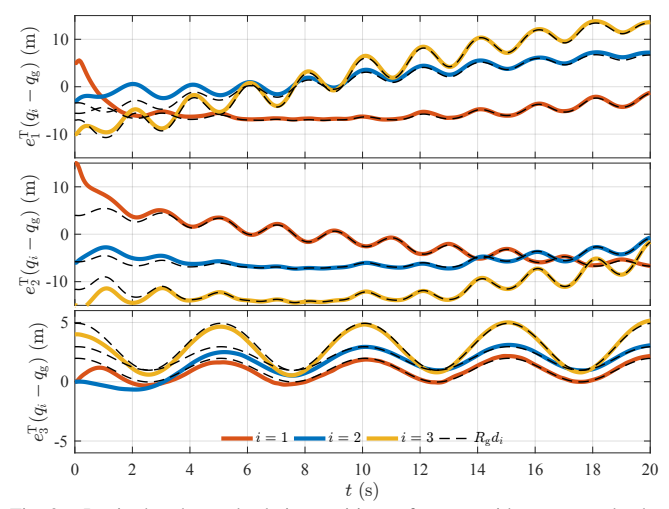


Fig. 2. Desired and actual relative positions of agents with respect to leader. Desired relative positions are achieved by approximately $t=10\ \mathrm{s}.$

of wind and with angle-of-attack and side-slip angles equal to zero, $\hat{\psi}_i = \psi_i$, $\hat{\theta}_i = \theta_i$, and $\hat{\phi}_i = \phi_i$.

We consider an aircraft equipped with an ArduPlane compatible autopilot that provides state estimates and accepts desired pitch angle $\hat{\theta}_{\mathrm{d},i}$, desired roll angle $\hat{\phi}_{\mathrm{d},i}$, and throttle T_i commands through the DroneKit Python API. For compatibility with the control inputs and feedback presented by the autopilot, we convert between the aircraft's angular velocity Ω and the Euler angle derivatives $\dot{\phi}_i$, $\dot{\phi}_i$, $\dot{\psi}_i$.

A. Formation Control Implementation

The aircraft described in above does not have the dynamics given by (1)–(3). However, we implement middle-loop controllers so the closed-loop UAV dynamics approximate the agent dynamics (1)–(3).

We use a PID controller with feedforward to command a pitch angle $\hat{\theta}_{\mathrm{d},i}(t)$ such that the course angle θ_i tracks the desired course angle $\theta_{\mathrm{d},i} \triangleq \arcsin{-e_3^\mathrm{T} p_{\mathrm{d},i}/s_{\mathrm{d},i}}$.

We assume the aircraft makes coordinated turns, and use the resulting kinematic equation to command a roll angle $\hat{\phi}_{d,i}$ from the desired heading rate $\dot{\psi}_{d,i}$. Specifically,

$$\hat{\phi}_{d,i}(t) = \arctan\left(\frac{\dot{\psi}_{d,i}(t)s_i(t)}{g}\right)\cos\hat{\theta}_i(t),$$

where $g = 9.81 \text{ m/s}^2$ and $\dot{\psi}_{\mathrm{d},i}$ is computed from (7).

We use a PID controller with feedforward to command the throttle T_i such that s_i tracks u_i . This controller is tuned such that the closed-loop speed dynamics from u_i to s_i approximate a first-order low-pass filter that can be written in the form (2), where $f_i(R_i,s_i)=-a_is_i$ and $g_i(R_i,s_i)=a_i$. The controller also has provisions to keep the airspeed inside the flight envelope of the aircraft.

B. Software-in-the-Loop Simulation Results

We present software-in-the-loop (SITL) simulation results using the formation-controller and middle-loop controllers described above. In these simulations, one instance of the Python implementation of the algorithm is run for each UAV, and it communicates with a corresponding instance of the

ArduPlane firmware running on a PC. These firmware instances communicate with corresponding JSBSim simulations of the JSBSim default aircraft model, Rascal110. All software runs on a single virtual Ubuntu machine.

For all examples in this section, let n=2 agents, and m=3. Let $f_i(s_i,R_i)=-0.4s_i$ and $g_i(s_i,R_i)=0.4$, which implies that the speed dynamics are a low-pass filter with unity gain at dc. The time constant 0.4 is estimated from the closed-loop step response of the UAV with the middle-loop speed controller. The desired positions are $d_1=[-10\quad 10\quad 0]^{\rm T}$ m, $d_2=[-10\quad -10\quad 0]^{\rm T}$ m. Let $\alpha_i=0.35,\ \beta_{12}=\beta_{21}=0.1,\ \gamma_i=1,\ \eta_i=0.001,$ and let $T_{\rm s}=0.1$ s, and $\phi_{\rm g}(t)\equiv 0.$

Example 3. The leader moves to a location away from the launch site and loiters in a 120m radius circle. The agents start from circling the launch site and enter formation. Figure 3 shows the trajectories of the leader and agents in the e_1 – e_2 plane plotted with time as the vertical axis, and Figure 4 shows $R_{\rm g}d_i$ and $q_i-q_{\rm g}$. The relative positions converge to

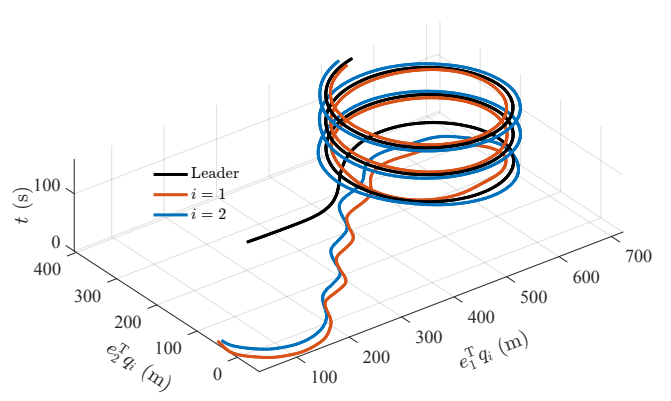


Fig. 3. Trajectories of leader and agents with time as the vertical axis. The agents converge to the desired relative positions at approximately $t=70~\mathrm{s}$.

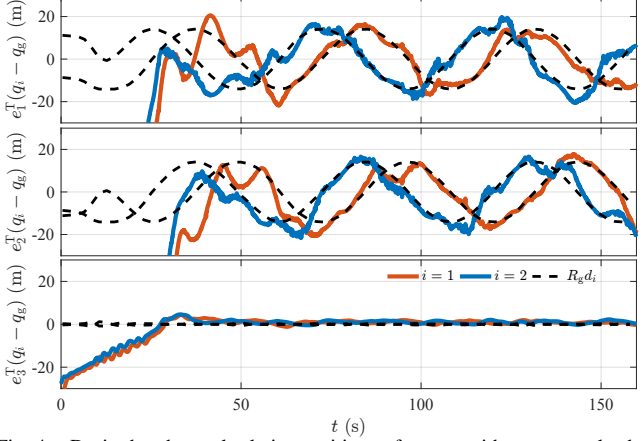


Fig. 4. Desired and actual relative positions of agents with respect to leader. Desired relative positions are achieved by approximately t = 70 s.

Example 4. The leader moves in a square pattern. The agents start from circling the launch site and enter formation. Figure 5 shows the trajectories of the leader and agents in the e_1 - e_2 plane plotted with time as the vertical axis, and Figure 6 shows $R_{\rm g}d_i$ and q_i - $q_{\rm g}$ Note that the desired position is approximately maintained through the abrupt turns in the

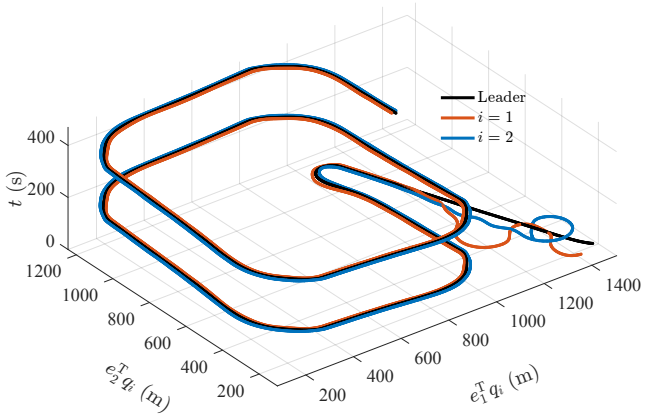


Fig. 5. Trajectories of leader and agents with time as the vertical axis. The agents converge to the desired relative positions at approximately $t=60~\mathrm{s}$.

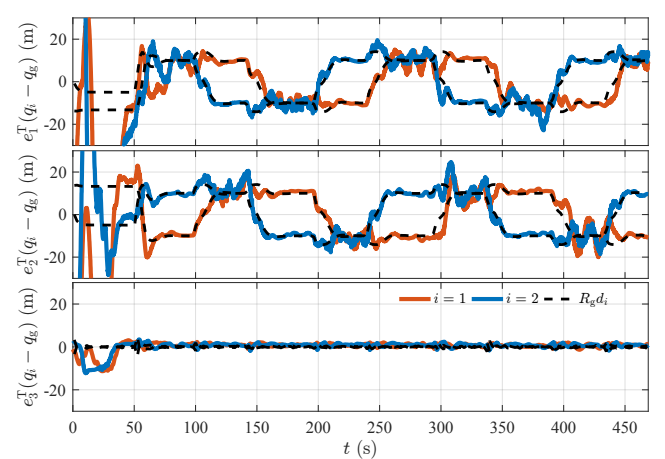


Fig. 6. Desired and actual relative positions of agents with respect to leader. Desired relative positions are achieved by approximately $t=60~\mathrm{s}$.

REFERENCES

- G. Punzo, P. Karagiannakis, D. J. Bennet, M. Macdonald, and S. Weiss, "Enabling and exploiting self-similar central symmetry formations," *IEEE Trans. Aerosp. Electron. Syst.*, vol. 50, no. 1, pp. 689–703, 2014.
- [2] R. W. Beard, T. W. McLain, D. B. Nelson, D. Keingston, and D. Johnson, "Decentralized cooperative aerial surveillance using decentralized cooperative aerial surveillance using fixed-wing miniature UAVs," *Proc. IEEE*, vol. 94, no. 7, pp. 1306–1324, 2006.
- [3] G. Lafferriere, A. Williams, J. Caughman, and J. J. P. Veerman, "Decentralized control of vehicle formations," Syst. Contr. Lett., vol. 54, no. 9, pp. 899–910, 2005.
- [4] W. Ren, "On consensus algorithms for double-integrator dynamics," IEEE Trans. Autom. Contr., vol. 53, no. 6, pp. 1503–1509, 2008.
- [5] Y. Cao and W. Ren, "Distributed coordinated tracking with reduced interaction via a variable structure approach," *IEEE Trans. Autom. Contr.*, vol. 57, no. 1, pp. 33–48, 2012.
- [6] Y. Zhang and Y. P. Tian, "Consensus of data-sampled multi-agent systems with random communication delay and packet loss," *IEEE Trans. Autom. Contr.*, vol. 55, pp. 939–943, April 2010.
- [7] H. G. Tanner, "Flocking with obstacle avoidance in switching networks of interconnected vehicles," in *Proc. IEEE Int. Conf. Robot. Automat.*, pp. 3006–3011, 2004.
- [8] B. J. Wellman and J. B. Hoagg, "A flocking algorithm with individual agent destinations and without a centralized leader," Sys. Contr. Lett., vol. 102, pp. 57–67, 2017.
- [9] D. Panagou, D. M. Stipanovi, and P. G. Voulgaris, "Distributed coordination control for multi-robot networks using Lyapunov-like barrier functions," *IEEE Trans. Autom. Contr.*, vol. 61, no. 3, pp. 617– 632, 2016.
- [10] R. Olfati-Saber, "Flocking for multi-agent dynamic systems: Algorithms and theory," *IEEE Trans. Autom. Contr.*, vol. 51, pp. 401–420, 2006.

- [11] D. V. Dimarogonas, S. G. Loizou, K. J. Kyriakopoulos, and M. M. Zavlanos, "A feedback stabilization and collision avoidance scheme for multiple independent non-point agents," *Automatica*, vol. 42, no. 2, pp. 229–243, 2006.
- [12] H. G. Tanner, A. Jadbabaie, and G. J. Pappas, "Flocking in fixed and switching networks," *IEEE Trans. Autom. Contr.*, vol. 52, no. 5, pp. 863–868, 2007.
- [13] D. Gu and Z. Wang, "Leader-follower flocking: Algorithms and experiments," *IEEE Trans. Contr. Sys. Tech.*, vol. 17, no. 5, pp. 1211– 1219, 2009.
- [14] H. Shi, L. Wang, and T. Chu, "Flocking of multi-agent systems with a dynamic virtual leader," *Int. J. Contr.*, vol. 82, no. 1, pp. 43–58, 2009.
- [15] H. Su, X. Wang, and Z. Lin, "Flocking for multi-agents with a virtual leader," *IEEE Trans. Autom. Contr.*, vol. 54, no. 2, pp. 293–307, 2009.
- [16] M. M. Zavlanos, M. B. Egerstedt, and G. J. Pappas, "Graph-theoretic connectivity control of mobile robot networks," *Proc. IEEE*, vol. 99, no. 9, pp. 1525–1540, 2011.
- [17] M. Guo, M. M. Zavlanos, and D. V. Dimarogonas, "Controlling the relative agent motion in multi-agent formation stabilization," *IEEE Trans. Autom. Contr.*, vol. 59, no. 3, pp. 820–826, 2014.
- [18] R. Olfati-Saber, J. A. Fax, and R. M. Murray, "Consensus and cooperation in networked multi-agent systems," *Proc. IEEE*, vol. 95, no. 1, pp. 215–233, 2007.
- [19] W. Ren, R. W. Beard, and E. M. Atkins, "Information consensus in multivehicle cooperative control," *IEEE Contr. Sys. Mag.*, vol. 27, no. 2, pp. 71–82, 2007.
- [20] Y. Cao, W. Yu, W. Ren, and G. Chen, "An overview of recent progress in the study of distributed multi-agent coordination," *IEEE Trans. Industrial Informatics*, vol. 9, no. 1, pp. 427–438, 2013.
- [21] Y. Gu, B. Seanor, G. Campa, M. R. Napolitano, L. Rowe, S. Gururajan, and S. Wan, "Design and flight testing evaluation of formation control laws," *IEEE Trans. Contr. Sys. Tech.*, vol. 14, pp. 1105–1112, 2006.
- [22] M. Turpin, N. Michael, and V. Kumar, "Trajectory design and control for aggressive formation flight with quadrotors," *Autonomous Robots*, vol. 33, pp. 143–156, 2012.
- [23] C. Park, N. Cho, K. Lee, and Y. Kim, "Formation flight of multiple uavs via onboard sensor information sharing," *Sensors*, vol. 15, pp. 17398– 17419, 2015.
- [24] V. Darbari, S. Gupta, and O. P. Verma, "Dynamic motion planning for aerial surveillance on a fixed-wing UAV," in *Proc. Int. Conf. Unmanned Aircrat Systems*, (Miami, FL), pp. 488–497, June 2017.
- [25] H. G. de Marina, Z. Sun, M. Bronz, and G. Hattenberger, "Circular formation control of fixed-wing uavs with constant speeds," in *Proc. IEEE/RSJ Int. Conf. Intelligent Robots and Sys.*, (Vancouver, Canada), pp. 5298–5303, September 2017.
- [26] B. J. Wellman and J. B. Hoagg, "Sampled-data flocking with application to unmanned rotorcraft," in *Proc. AIAA Guid. Nav. Contr. Conf.*, AIAA-2018-1856, (Kissimmee, FL), January 2018.
- [27] D. M. Stipanovi, G. Inalhan, R. Teo, and C. J. Tomlin, "Decentralized overlapping control of a formation of unmanned aerial vehicles," *Automatica*, vol. 40, no. 8, pp. 1285–1296, 2004.
- [28] C. B. Low, "A dynamic virtual structure formation control for fixed-wing uavs," in *Proc. IEEE Int. Conf. Contr. Automation*, (Santiago, Chile), pp. 627–632, December 2011.
- [29] M. Zhang and H. H. T. Liu, "Formation flight of multiple fixed-wing unmanned aerial vehicles," in *Proc. Amer. Contr. Conf.*, (Washington, D.C.), pp. 1614–1619, June 2013.
- [30] P. Panyakeow and M. Meshahi, "Deconflicted algorithms for a pair of constant speed unmanned aerial vehicles," *IEEE Trans. Aerosp. Electron. Syst.*, vol. 50, no. 1, pp. 456–476, 2014.
- [31] T. D. Barfoot and C. M. Clark, "Motion planning for formations of mobile robots," *Robotics Auton. Sys.*, vol. 46, pp. 65–78, 2004.
- [32] C. B. Low and D. Wang, "Gps-based tracking control for a car-like wheeled mobile robot with skidding and slipping," *IEEE/ASME Trans. Mechatronics*, vol. 13, no. 4, pp. 480–484, 2008.
- [33] R. W. Beard, J. Ferrin, and J. Humpherys, "Fixed wing uav path following in wind with input constraints," *IEEE Transactions on Control Systems Technology*, vol. 22, pp. 2103–2117, Nov 2014.
- [34] S. P. Bhat and D. S. Bernstein, "A topological obstruction to continuous global stabilization of rotational motion and the unwinding phenomenon," Sys. Contr. Lett., vol. 39, no. 1, pp. 63 70, 2000.
- [35] W. Song, J. Thunberg, X. Hu, and Y. Hong, "Distributed high-gain attitude synchronization using rotation vectors," *Journal of Systems Science and Complexity*, vol. 28, pp. 289–304, Apr 2015.